Guidance and Navigation for Solar Electric Interplanetary Missions

KENNETH H. ROURKE* AND JAMES F. JORDAN†
California Institute of Technology, Pasadena, Calif.

This paper makes a practical analysis of closed-loop guidance of a solar electrically thrusted interplanetary spacecraft. A first order guidance algorithm is used which allows easy interpretation yet rigorous treatment of trajectory terminal constraints. Interplanetary orbit determination is assumed to be provided by Earth-based radio (Doppler) tracking. Guidance and orbit determination is evaluated with respect to given trajectories and then combined to yield information on the encounter accuracies and guidance cost—in terms of additional power consumption, control deviations, and payload penalty—expected from given injection and thruster performance dispersions. The results are presented in terms of two representative cases: a Jupiter flyby/orbiter mission and a comet rendezvous mission in the late 1970's.

Introduction

Problem Statement

THE use of continuous propulsion in interplanetary flight requires the application of new guidance analysis concepts. Although much effort has been devoted to trajectory analysis problems, particularly in the area of optimal open-loop control of continuously thrusting space vehicles, less attention has been devoted to the problems of determining the orbit of such vehicles travelling on long interplanetary missions and correcting the thrust program of the engine to compensate for observed deviations from the nominal trajectory.[1,2]

A change in approach from the least squares method, which has been successfully used for orbit determination problems associated with ballistic space trajectories, is required because of the presence of large random nongravitational forces which influence the trajectory and hence the DSN tracking data. These forces result primarily from errors in the magnitude of the thrust and the thrust orientation.

The powered flight guidance problem also involves a change in approach from the impulsive midcourse correction methods used for ballistic flight, since thrust is available over a longer period of time. In fact, for most efficient use of effort, it often is desirable to use most, or all, of the available thrust time to make trajectory correction.

This paper illustrates these new perspectives by obtaining feasible solutions to the navigation and guidance problems and then applying them to two representative solar electric missions: a Jupiter flyby/orbiter and a comet rendezvous in the late 1970's.

Method of Guidance

It is assumed that spacecraft guidance will be accomplished in two phases. The first and primary phase occurs while the electric engine is in operation, and involves powered flight tracking and changing the nominal thrust acceleration vector to guide the spacecraft in order to decrease the terminal trajectory errors. The second phase, which occurs later in the mission after the nominal engine operation has been terminated, involves ballistic tracking and then turning the engines back on to make trajectory corrections. This paper is primarily concerned with the phase 1 guidance procedures.

It is assumed that the primary consideration in performing guidance corrections is the terminal accuracy of the trajectory. Other spacecraft or mission parameters which have been optimized in the selection of the nominal trajectory are assumed to be relatively insensitive to small variations in the flight path. The secondary consideration in performing guidance corrections is the magnitude of the control deviations. In light of these priorities a first-order control technique is used in the analysis. A first-order technique is distinguished from the second-order or second-variation techniques[3–5] in that only terminal constraints need be met through the use of small, yet otherwise arbitrary controls. Second-order techniques involve an actual local reoptimization of the trajectory to arrive at the desired control correction, and as one would expect, the implementation of such techniques into hardware and software is considerably more complex. Often the increased sophistication results in only marginal cost savings, which is particularly true for reoptimizing fuel expenditure for low thrust spacecraft. Fuel losses for all the cases considered in this paper are negligible.

Guidance Modes

During the powered flight phase of the mission, guidance corrections are performed by changing the nominal thrust vector time history. Two distinctly different modes of changing the thrust vector time history are dealt with in this paper. The first mode of guidance, referred to as "mode 1" in subsequent discussions, involves varying both the thrust acceleration magnitude and the thrust direction to correct the trajectory. It is assumed in mode 1 that the engine operation is terminated at the nominal engine cutoff time. The second mode, "mode 2," involves varying only the thrust direction, while keeping the magnitude of the thrust acceleration, and hence the power consumption rate, at the nominal level. In mode 2, the engine cutoff time can be varied in order to satisfy the terminal trajectory constraints.

Guidance Strategy

Trajectory corrections are made at discrete prescribed times rather continuously. This is a simple but adequate extension of the method used for guiding today's ballistic spacecraft.

Presented as Paper 70-1152 at the AIAA 8th Electric Propulsion Conference, Stanford, Calif., August 31–September 2, 1970, submitted October 2, 1970; revision received June 14, 1971.

Index categories: Spacecraft Navigation, Guidance, and Flight-Path Control Systems; Electric and Advanced Space Propulsion.

* Research Engineer, Estimation Theory Group, Tracking and Orbit Determination Section, Jet Propulsion Lab.

† Group Supervisor, Precision Orbit Determination Group, Tracking and Orbit Determination Section, Jet Propulsion Lab.

The sequencing of the tracking-estimation-correction scheme can be outlined as follows: 1) Obtain Earth-based Doppler tracking data prior to some specified guidance correction time t_1, and process the data using methods discussed in Refs. 6 and 7 to obtain an estimate of the vehicle state at the prescribed time t_1. 2) Using linear perturbation theory, calculate the change in the control program (electric thrust acceleration vector) during the time interval $t_1 \rightarrow t_c$ (the engine cutoff time) needed to drive the terminal state deviations to zero. 3) Obtain tracking data at a second correction time t_2, and repeat the estimation-correction process, . . .

It should be noted that this paper does not deal with the problem of optimizing the correction times. However, the correction times are chosen so as to yield reasonably small control deviations with near-minimum terminal trajectory errors.

Solar Electric Spacecraft Assumptions

Thruster Power

During the powered flight phase of a solar electric mission, the electric engines will be designed to consume less power than will be nominally available from the solar arrays. This is to allow for variation in the available jet power, P_j‡, due to 1) the solar power array interactions with the environment (i.e., particle impact, etc.) and 2) uncertainties in array performance. Operation of the engines at a power level below the nominal power output should allow additional power consumption for guidance purposes.

Thrust Acceleration

The instantaneous thrust acceleration magnitude is related to the engine parameters as follows

$$a(t) = F(t) \Big/ \left\{ M_o - \int_{t_o}^{t} \beta(\tau) d\tau \right\} \tag{1}$$

where $F(t)$ is the thrust magnitude given by the following equation

$$F(t) = \beta(t) c \tag{2}$$

and M_o is the spacecraft total mass at launch, $\beta(t)$ is the propellant fuel mass flow rate, and c is the effective exhaust velocity.

The jet power consumed by the engines is defined by

$$P_j = \beta c^2/2 \tag{3}$$

thus the thrust acceleration can be related to the consumed power by the relation

$$a(t) = 2P_j/Mc \tag{4}$$

Adjustments of the engine operation to the changing jet power are accomplished by variation of the mass flow rate β, while c is held constant throughout the mission. Thus, if the guidance of the vehicle demands variation in the acceleration magnitude, both instantaneous jet power and mass flow are directly affected, and spacecraft mass is ultimately changed.

Thrust Orientation Angles

The thrust orientation is assumed to be free to vary throughout the powered flight phase. Variations in the in-ecliptic-plane orientation angle Γ (defined from the sun-probe line) can be accomplished by directing the engine array, while variation in the out-of-plane angle λ can be performed by a total spacecraft rotation about the sun-spacecraft direction. The geometry of these angles is illustrated in Fig. 1.

Thrust Acceleration Vector and Equations of Motion

The thrust acceleration vector **a** has the following vector components in an ecliptic coordinate system:

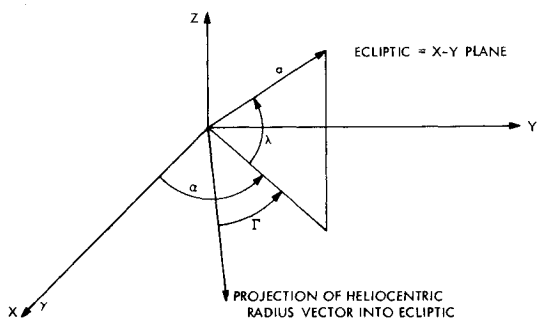

Fig. 1 Thrust vector geometry.

$$\begin{aligned} a_x &= a \cos\alpha \cos\lambda \\ a_y &= a \sin\alpha \cos\lambda \\ a_z &= a \sin\lambda \end{aligned} \tag{5}$$

and the nominal equation of motion of the spacecraft during the powered flight heliocentric phase of a mission can be written as follows:

$$\dot{\mathbf{V}} = \mathbf{a} + \mathbf{f} \qquad \dot{\mathbf{X}} = \mathbf{V} \tag{6}$$

where **f** is a 3×1 vector which represents the acceleration of the probe due to the gravitational attraction of the sun, i.e.,

$$\mathbf{f}^T = [f_x, f_y, f_z]^T = -\mu/r^3 [X, Y, Z]^T \tag{7}$$

The in-ecliptic-plane orientation angle α (defined from the x axis) is related to Γ by $\alpha = \Gamma + \theta$, $\theta = \tan^{-1}(Y/X)$.

Representative Solar Electric Missions

Guidance results will be presented for two representative solar electric missions in the late 1970's time frame. The first mission is a Jupiter flyby/orbiter mission, and the second is a d'Arrest Rendezvous mission. A detailed study of a Jupiter flyby mission for launch in 1976 is presented in Ref. 8, while a cursory examination of a rendezvous missions with Comte d'Arrest is given in Ref. 9. The trajectory characteristics of the two missions are given in the following paragraphs.

Jupiter Mission

The Jupiter mission trajectory is representative, for guidance study purposes, of the type that a solar electric flyby or orbiter mission would require. In the case of an orbiter mission, planetary capture is accomplished by a high thrust (chemical) retro burn. The projection of the flight path in

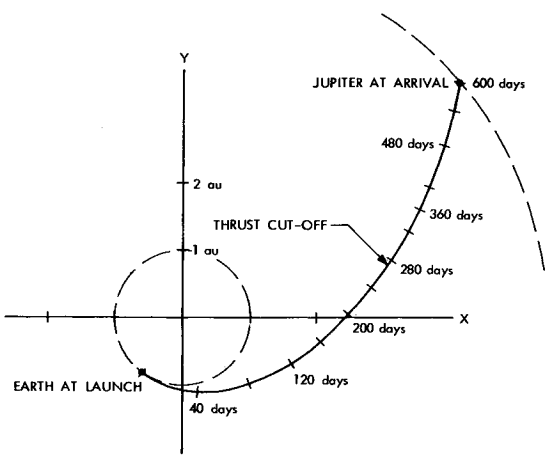

Fig. 2 Jupiter orbiter/flyby reference trajectory profile.

‡ Jet power and electrical power are assumed equal here.

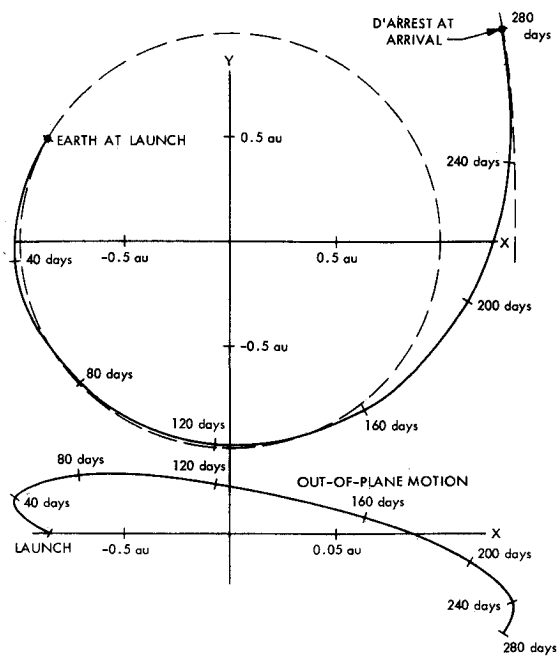

Fig. 3 d'Arrest rendezvous reference trajectory profile.

the ecliptic plane is illustrated in Fig. 2. The flight time is 600 days, and the engine operation is terminated 272 days after launch, when the spacecraft is 3 a.u. from the sun.

d'Arrest Mission

As an example of an orbit rendezvous mission, a trajectory to Comet d'Arrest in 1976 has been chosen. The projection of the flight path in the ecliptic plane and the projection of the flight path out of the ecliptic plane are illustrated in Fig. 3. The engine is operated for the entire duration of the mission, which is 280 days.

Theoretical Development

Trajectory Accuracy Analysis

Consider a solar-electrically thrusted spacecraft travelling on an interplanetary trajectory. The accuracy of the trajectory is adversely affected by both injection velocity (launch vehicle) errors and random forces continually acting on the spacecraft while the electric engine is operating. These forces result from uncertainties in the regulation of the engine behavior itself, i.e., errors in the regulation of the magnitude and direction of the thrust acceleration. These errors, with their respective one-sigma magnitudes, are: 1) High- and low-frequency variations in the regulation of the beam current and beam voltage (1%). 2) Low-frequency variation in the regulation of the mass flow rate (5%). 3) High-frequency variation in the thrust direction due to attitude control limit cycle (1°). 4) Constant errors in thrust orientation due to engine grid misalignments (2°). 5) Initial velocity errors at Earth injection (3.0 m/sec for the Titan III-D (1205)/Centaur Launch Vehicle).

Simulation of Random Accelerations

In this paper the random accelerations resulting from the variations in spacecraft performance are modeled conservatively as exponentially correlated Gaussian noise. If the components of the noise are assumed uncorrelated with each other, and the noise is assumed spherically distributed, then the autocorrelation function can be stated as:

$$E[\mathbf{n}(t_1)\mathbf{n}(t_2)^T] = R(t_1,t_2) = \sigma_\eta^2 e^{-1/\tau(|t_1-t_2|)} I_{3\times 3} \qquad (8)$$

where: $\mathbf{n}(t)$ is the 3×1 acceleration vector, σ_η is the standard deviation of the components of $\mathbf{n}$. τ is the correlation time, and $I_{3\times 3}$ is a 3×3 identity matrix.

Spacecraft Equation of Motion

The spacecraft state (position and velocity) can be generated by a solution to the following set of stochastic differential equations:

$$\dot{\mathbf{x}} = F\mathbf{x} + \mathbf{n}$$

where $\mathbf{x}$ is a 6×1 vector of state (velocity and position) deviations from the nominal, or reference, trajectory, i.e.,

$$\text{and} \quad F = \begin{bmatrix} 0 & \dfrac{\partial(f_x,f_y,f_z)}{\partial(x,y,z)} \\ I_{3\times 3} & 0 \end{bmatrix} \qquad (9)$$

Open-loop Covariance Matrix of the Errors in State

The trajectory accuracy is described by the open-loop covariance matrix of the errors in the state due to the initial velocity errors and the continuous acceleration errors experienced by the space vehicle. If the motion of the spacecraft about the nominal trajectory obeys Eq. 9, then the time history of the 6×6 covariance matrix of errors in position and velocity, i.e., $P(t) = e[\mathbf{x}(t)\mathbf{x}(t)^T]$, can be found from the following expression

$$P(t) = \phi_{xx}(t,t_o)P_o\phi_{xx}^T(t,t_o) + \int_{t_o}^{t}\int_{t_o}^{t} \times \phi_{xx}(t,\tau)\tilde{R}(\tau,\rho)\phi_{xx}^T(t,\rho)d\tau d\rho \qquad (10)$$

where

$$\underset{6\times 6}{\tilde{R}}(\tau,\rho) \begin{bmatrix} R(\tau,\rho)_{3\times 3} & 0 \\ 0 & 0 \end{bmatrix}$$

P_o is the initial open-loop covariance matrix due to launch vehicle injection errors, and $\phi_{xx}(t,t_o)$ is the state transition matrix, which has the following properties:

$$\dot{\phi}_{xx}(t,t_o) = F(t)\phi_{xx}(t,t_o), \quad \phi_{xx}(t_o,t_o) = \underset{6\times 6}{I} \qquad (11)$$

Accuracy Results for an Unguided Trajectory

The open-loop trajectory errors for the Jupiter and d'Arrest missions are computed using Eq. 10 and assuming: 1) the standard deviation of the spherical random acceleration errors are 1% of the time varying low-thrust acceleration magnitude, 2) the correlation time is 1000 sec, and 3) the a priori covariance matrix of the state errors representative of Titan III-D (1205)/Centaur launch vehicle, i.e., 3.0 m/sec.

For the Jupiter Mission the final position error at the planet encounter is 475,000 km, while for the d'Arrest Mission the terminal accuracy is 167,000 km. Thus, large trajectory dispersions occur at the target arrival time for both missions, which lead to unnecessarily large corrections to the flight path if only a chemical midcourse engine is used for guidance. The requirement for intermittant monitoring of the thrusting program is indicated by these results, with guidance corrections being performed in accordance with an orbit determination procedure.

Orbit Determination of the Spacecraft

In this presentation state information will be obtained from an orbit determination procedure which incorporates Earth-based Doppler (range rate) measurements. The trajectory accuracy conditioned on the information gained from the tracking data can be derived from Eq. (10), if augmented with terms expressing the information content of the tracking data. In this study, the Doppler information is taken over three successive tracking station passes at 16 day intervals during

the powered flight portion of the trajectory. The covariance matrix of the spacecraft velocity and position errors along the trajectory, where errors are now taken as the difference between the true state and the minimum variance estimate of the state, undergoes the following reductions at the times at which range rate measurements $\dot{\rho}$ are taken

$$\hat{P}(t) = \bar{P}(t) - \bar{P}H^T[H\bar{P}H^T + R']^{-1}H\bar{P} \qquad (12)$$

where 1) $\hat{P}(t) = E[(\mathbf{x}(t) - \hat{\mathbf{x}}(t))(\mathbf{x}(t) - \hat{\mathbf{x}}(t)^T)]$, $\hat{\mathbf{x}}(t)$ being the minimum variance estimate of the state variable $\mathbf{x}(t)$, given a measurement of time t. 2) $\bar{P} = E[(\mathbf{x} - \bar{\mathbf{x}})(\mathbf{x} - \bar{\mathbf{x}})^T]$, $\bar{\mathbf{x}}$ being the minimum variance estimate of $\mathbf{x}(t)$, given measurements made prior to the time t. 3) $H = \partial(\dot{\rho})/\partial(u,v,w,x,y,z)$, and 4) $R' = \sigma_e^2$, where σ_e is the standard deviation of the noise in a range-rate measurement.

The new minimum variance estimate of the state deviation is related to the prior estimate by the following equation

$$\hat{\mathbf{x}}(t) = \bar{\mathbf{x}}(t) + \hat{P}(t)H^TR'^{-1}[\delta\dot{\rho}(t) - H\bar{\mathbf{x}}(t)]$$

where $\delta\dot{\rho}$ is the difference between the actual and nominal range rate observables.

Accuracy Results in the Presence of Earth-Based Counted Doppler Measurements

The time histories of the root-sum-square standard deviations of the error in the estimates of the velocity and position of the spacecraft are shown respectively in Fig. 4 for the Jupiter and d'Arrest Missions. The standard deviation of the error in the range rate measurements is taken as 1 mm/sec, and the measurements are taken at 1 min time intervals.

For the Jupiter mission, the estimated position uncertainty at the end of the powered flight phase is 3800 km while the velocity uncertainty is 0.27 m/sec. These state uncertainties, when mapped to Jupiter encounter, yield a final *rss* position error of 9700 km. For the d'Arrest mission the final estimated position uncertainty is 5400 km. The uncertainties are indicative of the best accuracy achievable with phase 1 guidance. Note that the position uncertainty level for the estimated state has dropped by roughly two orders of magnitude from the open-loop accuracies.

Spacecraft Control

In this study a control maneuver will be performed at a specific time, by adjusting the thrust program according to the results of the state estimation procedure discussed in the previous section. It is assumed that the primary consideration in performing guidance corrections is the terminal accuracy and the secondary consideration is the magnitude of the control deviations. For this reason, full control corrections are performed, that is, the observed control is computed to drive the observed state deviations to zero at the target arrival time. No effort is extended to drive the state back to the nominal before the arrival time.

If a guidance correction has been performed by perturbing the control variables then the behavior of the particular trajectory relative to the nominal trajectory can be described by the following linear differential equation:

$$\dot{\mathbf{x}} = F\mathbf{x} + G\mathbf{u} \qquad (13)$$

where

$$\underset{3\times 6}{G} = [\partial(a_x,a_y,a_z)/\partial(a,\alpha,\lambda)\,|\,0]$$

and

$$\mathbf{u}^T = [\delta a/a, \delta\alpha, \delta\lambda]$$

It is desired to control the spacecraft such that the control deviations are small. One way to insure this is to use a control law which minimizes some function or functional of the control deviations. Here, the following functional of control

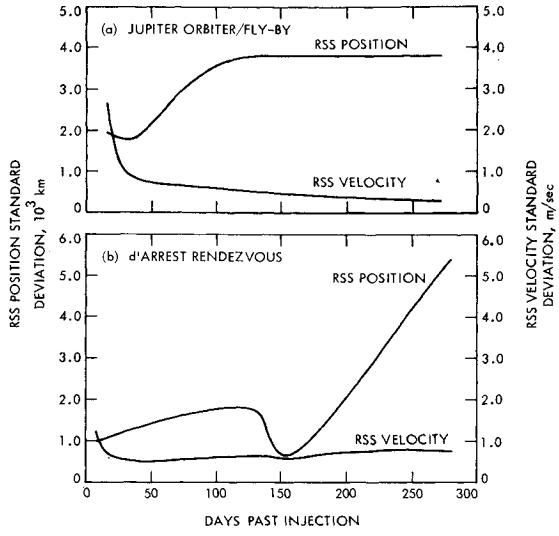

Fig. 4 Estimated velocity and position uncertainty time histories.

deviations is minimized.

$$J = \tfrac{1}{2}\int_{t_1}^{t_c} \mathbf{u}^T W \mathbf{u} dt \qquad (14)$$

where $\underset{3\times 3}{W}$ can be chosen as any positive definite symmetric weighting matrix. This approach parallels that presented initially in Ref. 5.

In order to determine the functional form of the control, J is minimized subject to the constraint that Eq. (13) be satisfied at all points along the trajectory between t_1 and t_c. Trajectory terminal constraints are given in terms of a set of $r(r \times 6)$ linear relations of the terminal state variables, i.e.,

$$K\phi_{xx}(t_f,t_c)\mathbf{x}(t_c) = 0 \qquad (15)$$

where K is an $r \times 6$ matrix and $\mathbf{x}(t_c)$ is the spacecraft state at time of thrust cutoff. Equation (15) admits a large variety of specific terminal constraints including: fixed time rendezvous, where position and velocity are constrained ($K = I_{6\times 6}$), and fixed time flyby where only position is constrained ($K = [0\,|\,I_{3\times 3}]$). Variable encounter time and variable approach direction constraints may also be treated with the proper choice of K.

The constrained problem is solved in terms of an adjoined functional

$$J = \mathbf{v}^T K\phi_{xx}(t_f,t_c)\mathbf{x}(t_c) + \int_{t_1}^{t_c} \mathbf{u}^T W\mathbf{u} + \lambda^T(\dot{\mathbf{x}} - F\mathbf{x} - G\mathbf{u})dt \qquad (16)$$

where $\lambda(t)$ is a vector of time varying Lagrange multipliers and $\mathbf{v}$ is an r-dimensional vector of constant multipliers.

The solution to the minimization problem can be carried out by the standard calculus of variations technique and can be stated in terms of the following six-dimensional Euler-Lagrange equation:

$$\frac{d}{dt}\begin{bmatrix}\mathbf{x}\\ \lambda\end{bmatrix} = \left[\begin{array}{c|c} F & GW^{-1}G^T \\ \hline 0 & -F^T \end{array}\right]\begin{bmatrix}\mathbf{x}\\ \lambda\end{bmatrix} \qquad (17)$$

where the control deviation vector is related to the vector of Lagrange multipliers by the following relation:

$$\mathbf{u} = W^{-1}G^T\lambda \qquad (18)$$

The set of $2n$ differential equations is constrained by the $2n$ boundary point conditions:

at t_1: $$\mathbf{x}(t_1) = \hat{\mathbf{x}}(t_1) \qquad (19)$$

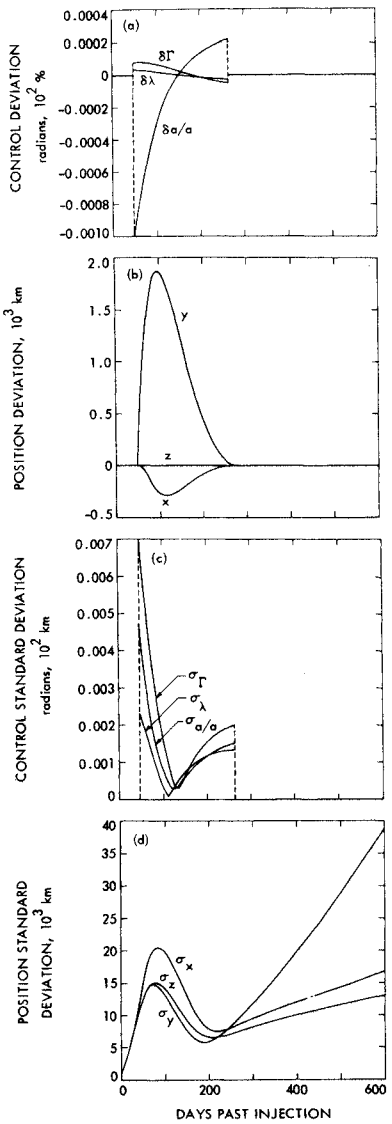

Fig. 5 Jupiter 48 day mode-1 return to nominal correction.

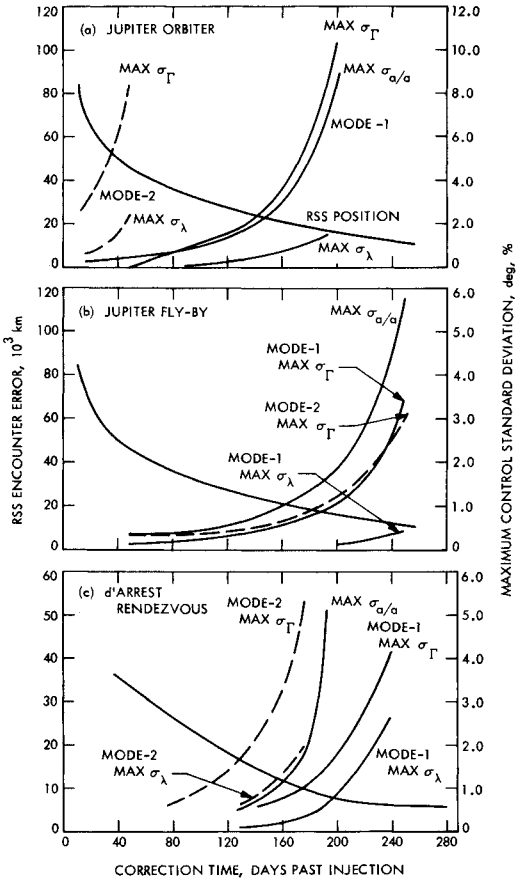

Fig. 6 Sensitivity of control excursion and encounter errors to correction time.

and at t_c: $K\phi_{xx}(t_f,t_c)\mathbf{x}(t_c) = 0 \qquad \lambda(t_c) = K^T\nu$

The solution to Eq. (17) can be stated as

$$\begin{aligned}\mathbf{x}(t) &= \phi_{xx}(t,t_1)\hat{\mathbf{x}}(t_1) + \phi_{x\lambda}(t,t_1)\lambda(t_1)\\ \lambda(t) &= \phi_{\lambda\lambda}(t,t_1)\lambda(t_1)\end{aligned} \tag{20}$$

where the 12×12 generalize state transition matrix

$$\phi = \begin{bmatrix}\phi_{xx} & \phi_{x\lambda}\\ 0 & \phi_{\lambda\lambda}\end{bmatrix}$$

has the following properties

$$\dot{\phi}(t,t_1) = \begin{bmatrix}F & GW^{-1}G^T\\ 0 & -F^T\end{bmatrix}\phi(t,t_1) \tag{21}$$

and

$$\phi(t_1,t_1) = \underset{12\times12}{I}$$

By evaluating Eq. (2) at t_c, and eliminating the vectors $\mathbf{x}(t_c)$, $\lambda(t_c)$ and ν from the equation, the initial Lagrange multiplier vector $\lambda(t_1)$ can be found in terms of the state estimate at t_1, $\hat{\mathbf{x}}(t_1)$, and the resulting state deviation and control can be stated as

$$\begin{aligned}\mathbf{x}(t) &= A(t,t_c,t_f,t_1)\hat{\mathbf{x}}(t_1)\\ \mathbf{u}(t) &= B(t,t_c,t_f,t_1)\hat{\mathbf{x}}(t_1)\end{aligned} \tag{22}$$

where

$$\underset{6\times6}{A} = \phi_{xx}(t,t_1) + \phi_{x\lambda}(t,t_1)D(t_c,t_f,t_1)$$

$$\underset{6\times6}{B} = W^{-1}G^T\phi_{\lambda\lambda}(t,t_1)D(t_c,t_f,t_1)$$

$$\underset{6\times6}{D} = \phi_{\lambda\lambda}{}^{-1}(t_c,t_1)\phi_{xx}{}^T(t_f,t_c)K^TC(t_c,t_f,t_1)K\phi_{xx}(t_f,t_1)$$

$$\underset{r\times r}{C} = [K\phi_{xx}(t_f,t_c)\phi_{x\lambda}(t_c,t_1)\phi_{\lambda\lambda}{}^{-1}(t_c,t_1)\phi_{xx}{}^T(t_f,t_c)K^T]^{-1}$$

Controls generated by the above technique are unique with respect to the weighting matrix W. The freedom to select W allows considerable flexibility in accomplishing spacecraft guidance, e.g., given control parameters can be restrained by adjusting the relative weights in W. For instance, mode 2 guidance is treated by zeroing the appropriate column of the G matrix at all times aside from nominal thrust switching times. At thrust switching (cutoff or restart) a Δa impulse is allowed by suitably adjusting W to account for switch time variations.

Statistics of the Controlled State Deviations and Control Deviations

It is assumed that the actual state deviations obey the following equation after a control correction $\mathbf{u}(t)$ has been made

$$\dot{\mathbf{x}} = F\mathbf{x} + G\mathbf{u} + \mathbf{n} \tag{23}$$

and hence the actual state deviations after a control correction at t_1 propagate by the following relation

$$\mathbf{x}(t,t_1) = A\hat{\mathbf{x}}(t_1) + \phi_{xx}(t,t_1)(\mathbf{x}(t_1) - \hat{\mathbf{x}}(t_1)) + \int_{t_1}^{t}\phi_{xx}(t,\tau)\mathbf{n}(\tau)d\tau \tag{24}$$

The covariance matrix of the difference between the actual

Table 1 Multicorrection policies achieving improved encounter accuracy

	Max $\sigma_{a/a}$	Max σ_Γ, deg	Max σ_λ, deg	σ_{t_c}, days	σ_m, kg	σ_{t_f}, days	σ_ϕ, deg	*Rss* pos. error, km	min *rss* pos. error, km
Jupiter orbiter									
Return to nominal mode 1[a]	2.2%	2.5	2.5	...	0.5	...	...	11,100	9,740
Free encounter time and approach asymptote 2[a]		0.52	0.11	1.1	0.8	0.12	0.02	11,100	9,740
Jupiter flyby									
Mode 2, corrections at 248 and 268 days		3.3	0.49	1.4	0.9	...	...	10,190	9,740
d'Arrest Rendezvous									
Mode 2, corrections at 152, 200, 248		2.9	0.27	0.04	0.02	...	...	5,980	5,370

[a] Corrections at 144, 224, and 248 days.

controlled state and the nominal state obeys the following propagation equation

$$P(t,t_1) = AP'(t_1)A^T + \phi_{xx}(t,t_1)\hat{P}(t_1)\phi_{xx}{}^T(t,t_1) + \int_{t_1}^{t}\int_{t_1}^{t} \phi_{xx}(t,\tau)\tilde{R}(\tau,\rho)\phi^T(t,\rho)d\tau d\rho, \quad (25)$$

and the control deviation itself is determined by Eq. (22) from the state estimate $\hat{\mathbf{x}}(t_1)$. Hence the covariance matrix of the control deviations propagates by the following equation

$$P_u(t,t_1) = BP'(t_1)B^T \quad (26)$$

where $P'(t_1) = E[\hat{\mathbf{x}}(t_1)\hat{\mathbf{x}}(t_1)^T]$, and can be shown to be equal to the difference between the open-loop state covariance matrix and the estimated state error covariance matrix, i.e.,

$$P'(t_1) = P(t_1) - \hat{P}(t_1) \quad (27)$$

Application to Representative Interplanetary Missions

Single Correction Policies

In the following sections the techniques that are developed previously are applied to the Jupiter orbiter, Jupiter flyby, and d'Arrest Rendezvous missions. The two Jupiter missions differ in terms of their terminal constraints: the orbiter requiring some form of velocity constraint at encounter and the flyby requiring no velocity constraint at encounter. As discussed previously, this treatment of guidance is concerned with sequences of discrete trajectory corrections. For clarity, the analysis is limited to as few such corrections as possible. The following accordingly begins with an example of a single correction guidance policy.

Figure 5 presents an example of a particular single guidance correction applied to the Jupiter orbiter mission. Shown are control and position deviations and associated statistics time histories for a 48 day return to nominal guidance correction. Figures 5a and 5b show the mode 1 control and corresponding state response to the correction of a 1 m/sec perturbation in the spacecraft y-velocity at 48 days past injection. Figures 5c and 5d present the statistical performance of the 48 day correction, in the form of control and position component standard deviations. The maximum expected excursion in the control variables for a particular guidance correction is of special importance in that a given spacecraft can be expected to have only a limited capacity to adjust the direction and magnitude of its thrust vector. In the case of the 48 day Jupiter trajectory correction, the maximum standard deviation in $\delta\Gamma$ and $\delta a/a$ are seen to be 0.007 rad (0.4°) and 0.47%, respectively. Note that the statistical uncertainties degrade the position accuracy relative to the reference trajectory to 10,000 km at thrust termination and 40,000 km at encounter. The large errors result from the early correction which permits state estimation uncertainties present at the correction time and subsequent thruster errors to propagate along the trajectory to produce large errors at encounter. Similar results can be given for the Jupiter flyby and d'Arrest missions.

Control effort and encounter accuracy for single correction guidance vary with the correction initiation time. Consider Fig. 6 which shows: 1) performance statistics, in the form of *rss* encounter positions errors and 2) guidance effort statistics in the form of maximum control excursion standard deviations obtained from individual single correction policies for varying correction times. Figure 6a presents mode 1 and mode 2 return-to-nominal policies for the Jupiter orbiter mission. Note how the required excursions, angles $\delta\Gamma$ and $\delta\lambda$ and relative acceleration $\delta a/a$ increase dramatically while *rss* encounter errors falls off as correction times approach thrust termination. The encounter accuracy curve is extended beyond realistic correction times as it is meaningful for representing the performance of repeated guidance corrections, where "correction time" refers to the final correction time. The limiting accuracy for guidance is shown to be 9700 km corresponding to a guidance correction made near thrust termination. Mode 2 angle excursions are seen to be generally larger than those of mode 1, which is to be expected of the more constrained correction technique. Mode 1 and mode 2 angle excursions are comparable, however, in the case of the Jupiter flyby mission shown in Fig. 6b. Figure 6c displays similar results for d'Arrest mission.

Multicorrection Policies and Encounter Accuracy

Given specific control excursion tolerances it is often impossible to approach the limiting guidance accuracy with single correction policies. Therefore some form of multicorrection policy is required. The following simple strategy for selecting correction times is suggested. 1) The initial correction time is given by the lastest time for which a given control tolerance can be met. 2) The final correction time is given by the earliest time that required encounter accuracy can be attained. 3) Additional correction times may be inserted between the first and the last to insure the given control tolerances are met.

Table 1 presents four multicorrection policies based on a set of hypothetical tolerances and the above strategy. Included in the table are control effort figures of merit in the form of maximum $\delta\Gamma$ and $\delta\lambda$ standard deviations, the corresponding thrust termination time standard deviations σ_{t_c}, and the expected mass loss σ_m. The standard deviations of arrival time and approach asymptote direction variations are σ_{t_f} and σ_ϕ, respectively. The second Jupiter orbiter example utilizes mode 2 corrections satisfying a relaxed terminal constraint. The resulting control effort is reduced while the encounter time varies by only 3 hr. This example shows that a sufficiently relaxed terminal constraint can be met with small, (or late) control corrections. Note that in all cases mass loss is very low.

Phase 2 Guidance Analysis

In this paper emphasis is given to phase 1 guidance, i.e., prethrust termination guidance. The major limitation on

Table 2 Accuracies and cost of a vernier correction made 60 days after nominal thruster cutoff time (thrust acceleration magnitude = 0.5×10^{-4} m/sec^2)

	With phase 1 guidance	Without phase 1 guidance
Rss o.d. accuracies at the time of vernier correction ($t_c + 60$ days)	$\sigma_v = 3$ cm/sec $\sigma_x = 800$ km	$\sigma_v = 3$ cm/sec $\sigma_x = 800$ km
Engine operation duration for vernier correction	18 hr	5 days
Rss position error at encounter	2000 km	10,000 km

this form of guidance is imposed by the diminished state estimation capacity that results from the noisy spacecraft dynamics. In the case of the Jupiter missions, performance is limited to 10,000 km encounter error. Phase 2 guidance seeks to remedy the problem by allowing a vernier correction (see Ref. 10) to be made after an interval of post cutoff ballistic tracking is performed. The ballistic tracking is inherently more accurate than tracking before thrust cutoff and therefore, significant encounter error reductions may be realized. (Reference 7 includes a comparison of ballistic and powered flight radio navigation accuracies.) In the Jupiter missions, for instance, ballistic tracking for 60 days after thrust termination yields state estimation *rss* error reductions from 4,000 km and 50 cm/sec–800 km and 3 cm/sec, respectively.

Table 2 presents accuracy and cost results for two Jupiter mission (orbiter or flyby) phase 2 guidance corrections assuming the estimation reductions given above. One correction is assumed to be made after phase 1 guidance, while the other is made without phase 1 guidance, and hence in that case, all state errors that have accrued up to that time must be corrected. Correction ΔV's are, respectively, 0.3 and 20 m/sec. At 333 days past injection the low thrust acceleration is only 0.5×10^{-4} m/sec^2 so that 0.3 and 20 m/sec require 18 hours and 5 days of engine operation, respectively. The low-thrust engines do not operate perfectly and hence the vernier corrections produce state errors that affect accuracy at encounter. Nominal 1% acceleration errors produce 2000 km total error for phase 1 plus phase 2 guidance and 10,000 km for phase 2 guidance alone. Thus in this case, phase 2 guidance alone is not better than phase 1 guidance alone, whereas the two techniques used together provide significantly improved encounter accuracy for the Jupiter mission. The analysis of phase 2 guidance is idealized in that ΔV corrections in all directions are assumed possible.

Summary and Conclusions

This paper applies the techniques of linear filter theory and quadratic cost linear control theory to the problem of guiding a solar electric powered spacecraft in interplanetary flight. The tools that are developed prove to be quite flexible in treating a variety of mission types and guidance strategies. Specific results are obtained through a study of guidance for two representative interplanetary trajectories: to Jupiter and comet d'Arrest.

The analysis of the Jupiter and d'Arrest trajectories indicate the following general results: 1) Guidance costs are small based on present-day launch vehicle and electric propulsion capability. This statement applies to a large variety of guidance mode—terminal constraint—correction sequence-combinations. 2) Near limiting accuracy (at encounter) can be attained through only a few guidance corrections to the thrust program. 3) Guidance performance during the powered phase of flight is definitely limited by orbit determination capability. 4) Phase 1 and phase 2 guidance are complementary techniques. Together they provide the accuracy associated with ballistic guidance and the low cost associated with low-thrust guidance.

References

[1] Friedlander, A. L. et al., "Error Analysis of Celestial-Inertial Navigation for Low Thrust Interplanetary Vehicles," Rept. 740, April 1967, NASA.

[2] Fraser, D. C. et al., "Guidance and Navigation Requirements for Unmanned Fly-By and Swingby Missions to the Outer Planets," Study Rept., Contract NAS 2-5043, May 1970, NASA.

[3] Kelley, J. H., "Guidance Theory and Extremal Fields," *Transactions on Automatic Control*, Institute of Radio Engineers, 1962, pp. 947–953.

[4] Breakwell, J. V., Speyer, J. L., and Bryson, A. E., "Optimization and Control of Nonlinear Systems Using the Second Variation," *Society for Industrial and Applied Mathematics Journal on Control*, Ser. A, Vol. 1, Nov. 1963, pp. 193–222.

[5] Bryson, A. E. and Denham, W. F., "Multivariable Terminal Control for Minimum Mean Square Deviation from Nominal Path," *Proceedings of the Institute of Aerospace Sciences Symposium on Vehicle Systems Optimization*, 1961, pp. 91–97.

[6] Kalman, R. E., "A New Approach to Linear Filtering and Prediction Problems," *Journal of Basic Engineering Transactions of American Society of Mechanical Engineers*, Vol. 82-D, 1960, pp. 35–45.

[7] Jordan, J. F., "Orbit Determination for Powered Flight Space Vehicles on Deep Space Missions," *Journal of Spacecraft and Rockets*, Vol. 6, No. 5, May 1969, pp. 545–551.

[8] Barber, T. A. et al., "1975 Jupiter Flyby Mission Using a Solar Electric Spacecraft," Unpublished Rept., Advanced Study Document 760-18, March 1968, Jet Propulsion Lab., Pasadena, Calif.

[9] Atkins, K. L., Jordan, J. F., and Sauer, C. G., "Solar Electric Prospects for d'Arrest Rendezvous," Interoffice Memo. 385-70-165, June 1970, Jet Propulsion Lab., Pasadena, Calif.

[10] Meisinger, H. F. et al., "Study of a Solar Electric Multi-Mission Spacecraft Final Summary Technical Report," Unpublished Rept., Jan. 1970, Thompson-Ramo-Wooldridge Systems Group, Redondo Beach, Calif.